

Boundary Conditions of the Heliosphere

P. C. Frisch

Department of Astronomy and Astrophysics, University of Chicago, Chicago, Illinois, USA

Abstract.

Radiative transfer equilibrium models of nearby interstellar matter (ISM) are required to determine the boundary conditions of the heliosphere from astronomical observations of nearby stars. These models are also constrained by data on the ISM inside of the solar system, including pickup ion, anomalous cosmic rays, and *in situ* He^o data. The two best ISM models give semi-empirical filtration factors for H (0.41 - 0.52), He (0.86–1.16), N (0.74–1.11), O (0.55–0.77), Ne (1.41–2.80), and Ar (0.61–1.76) when observational uncertainties are included. Uncertainties in the Ne filtration factor may result from poorly known interstellar abundances. These models predict the characteristics of the ISM outside of the solar system: $n(\text{H}^o)=0.20\text{--}0.21\text{ cm}^{-3}$, $n(e^-)=0.10\text{ cm}^{-3}$, $\text{H}^+/\text{H}=0.29\text{--}0.30$, and $\text{He}^+/\text{He}=0.47\text{--}0.51$. However, *if* the isotropic 2 kHz emission observed by Voyager (Kurth & Gurnett 2003) is formed in the surrounding ISM, an alternate model (Model 25) is indicated. The weakly polarized starlight of nearby stars suggests that the local galactic magnetic field is parallel to the galactic plane, and the strongest polarization is towards the upstream direction of the ISM flow, and also (coincidentally) near the ecliptic plane. Observations of nearby ISM, the radiative transfer models, and historical ¹⁰Be records provide information on past variations in the galactic environment of the Sun.

1. Introduction

The boundary conditions of the heliosphere are dominated by the ionization, density, temperature, and magnetic field of the surrounding interstellar cloud. The first use of anomalous cosmic ray (ACR) data to study interstellar ionization compared ACRs and the Mg^o/Mg⁺ ratio towards Sirius, relying on sightline-averaged ionization rates (Frisch 1994). Full radiative transfer equilibrium models of interstellar gas within ~ 3 pc are now available, predicting ISM properties at both the heliosphere boundary and averaged over sightlines towards nearby stars (Slavin & Frisch 2002, SF02, Frisch & Slavin 2003, FS03). Such models provide a tool for evaluating the boundary conditions of the heliosphere when constrained with interstellar matter (ISM) data inside and outside of the heliosphere. However, the loss of interstellar neutrals to charge exchange with interstellar ions in the heliosheath regions (“filtration”, Ripken & Fahr 1983, Izmodenov et al. 1999, Mueller & Zank 2002, Cummings & Stone 2002, CS02) must be considered when interpreting the *in situ* data. In this paper, the radiative model predictions for the physical properties of the ISM at the solar location are used to determine semi-empirical filtration factors, extending the discussion presented in FS03. Models consistent with a possible interstellar origin for the 2 kHz emission observed by Voyager in the outer heliosphere (Kurth & Gurnett 2003) are also discussed, along with evidence for a nearby interstellar magnetic field and time-variability of the boundary conditions of the heliosphere.

2. Why Radiative Transfer Models?

The ionization of the ISM at the solar location and boundary conditions of the heliosphere are highly sensi-

tive to the interstellar cloud properties integrated from the solar location (SoL) to the cloud surface. Since the H° column density to the local cloud surface is $\log N(H^{\circ}) < 18 \text{ cm}^{-2}$, and photons which ionize H ($>13.6 \text{ eV}$) and He ($>24.6 \text{ eV}$) are attenuated to $1/e$ by $\log N(H^{\circ}) \sim 17.2 \text{ cm}^{-2}$ and $\log N(He^{\circ}) \sim 17.7 \text{ cm}^{-2}$ respectively, the H° and He° densities at the SoL are sensitive to the radiation attenuation inside the cloud and to cloud geometry. The measurements which best distinguish the properties of the surrounding cloud are those which sample partially ionized elements with first ionization potentials in the range 13–25 eV (e.g. H, He, O, N, Ne, and Ar), which also constitute the parent population of pickup ions and anomalous cosmic rays.

Radiative transfer (RT) models of ISM near the Sun ($<3 \text{ pc}$) are required to predict the ionization of the ISM at the SoL. RT models have been constructed using measurements of the interstellar radiation field in the interval 300–3000 Å, a modeled conductive interface between nearby ISM and the hot plasma ($\sim 10^6 \text{ K}$) interior of the Local Hot Bubble, and the cloud composition determined from observations of ISM both inside and outside of the solar system (see SF02 and FS03). Free parameters in these models include the H° column density towards the cloud surface ($N(H^{\circ})$, which is not directly measured for the sightline used to constrain the models, $\epsilon \text{ CMa}$), the soft X-ray emission from the Local Bubble hot plasma (characterized by plasma temperature T_H), the interstellar magnetic field strength (B , which regulates conduction at the cloud boundary and the extreme ultraviolet radiation field, Slavin 1989), and cloud density ($n_H = n(H^{\circ}) + n(H^+)$). Sightline-averaged values of the relative ionizations of H and He in the ISM are found from observations of the He° ionization edge (504 Å) towards nearby white dwarf stars (40–100 pc), which are strong sources of radiation in this extreme ultraviolet (EUV) wavelength interval (e.g. Kimble et al. 1993, Vallergera 1996). These data generally sample sightlines with several blended clouds, and show a wide variation in ionization ($N(H^{\circ})/N(He^{\circ}) \sim 10\text{--}15$). The equilibrium models fitting the high He ionization seen in the EUV data require an excess of radiation in the 500 Å region, when compared to the soft X-ray data, and the variation of H°/He° with cloud depth requires radiative transfer models (e.g. Cheng & Bruhweiler 1990, Kimble et al. 1993, Vallergera 1996, SF02).

The initial set of 25 models was pared to seven “best” models (Frisch and Slavin 2003, FS03) by introducing recent astronomical data indicating gas-phase interstellar abundances of $O/H \sim 400 \text{ ppm}$ in long ($>700 \text{ pc}$) interstellar sightlines through predominantly diffuse clouds (Andre et al. 2002), since O and H ionizations are closely coupled by charge exchange. Data on Mg°/Mg^+ and C^{+*}/C^+ towards $\epsilon \text{ CMa}$ (Gry & Jenkins 2001) then indicated that Models 2, 8, and 18 provide the best match to astronomical data, and Model 11 is within uncertainties (FS03). FS03 compared these models with He data inside of the solar system, and concluded Models 2 and 8 are the best models if He is not filtered in the heliosheath regions. (Ionization and density predictions for the full 25 models are available at http://astro.uchicago.edu/~frisch/SlavinFrisch2002_tables.) The principal failures of these two RT models are that predicted Ne° densities are $\sim 50\%$ of Ne° densities inferred from PUIs and ACRs, and cloud temperatures are $\sim 30\%$ larger than values inferred from the He° data. The filtration predicted by these models is examined below.

3. Filtration Factors

Gloeckler & Geiss (2001, GG01) made an empirical estimate of hydrogen filtration, $F_H = [n_{TS}(H)/n_{TS}(He)]/\phi$, by comparing H and He densities at the termination shock with the interstellar values, $\phi = n_{IS,Sun}(H^{\circ})/n_{IS,Sun}(He^{\circ})$, assuming negligible He filtration. They assumed $\phi=11.25$ based on white dwarf data which show $N(H^{\circ})/N(He^{\circ})\sim 11.25$, yielding $F_H = 0.54$. GG01 also derived an O filtration factor $F_O = 0.62$, using H° and O° column densities towards the stars Procyon and Capella. (Volume densities are n , in units cm^{-3} , and column densities for element X are $N(X)$, in units cm^{-2}). The SF02 models show $N(H^{\circ})/N(He^{\circ})=8.8-13.6$, consistent with the large variations found for $N(H^{\circ})/N(He^{\circ})$ towards nearby stars, and predict values $\phi=12.1-14.7$ at the SoL. The relative H and He ionizations at the SoL depend on the model parameters ($\phi=\phi(n_H, N(H^{\circ}), B, T_H)$), since H-ionizing photons are attenuated more strongly than He-ionizing photons.

Filtration factors can be determined semi-empirically from comparisons between ionization predictions for the SoL (Table 7 in SF02) and *in situ* data on the byproducts of ISM interactions with the solar system. Neutral densities at the termination shock are determined from pickup ion (GG03), anomalous cosmic ray (CS02), and direct He measurements (Witte et al. 2003). These data give $n_{TS}(He^{\circ})=0.0145\pm 0.0015\text{ cm}^{-3}$ and $n_{TS}(H^{\circ})=0.095\pm 0.01\text{ cm}^{-3}$. The H and He filtration factors determined from the 25 models are shown in Fig. 1a, along with theoretical predictions of H and He filtration factors. The seven models with O/H \sim 400 ppm are plotted as filled circles, or triangles for models 2, 8, 18 which provide the best match to astronomical data. Among the three models best matching astronomical data, 2 and 8 are most consistent with predictions of negligible He filtration. The F_{He} predictions for the upstream direction are $F_{He}=0.98-0.99$ (Mueller and Zank, 2002) and $F_{He}=0.94$ (CS02). The hydrogen filtration factors are more uncertain, $F_H=0.4-0.5$ (Mueller & Zank 2002, Ripken & Fahr 1983, Izmodenov et al. 1999, Gloeckler & Geiss 2003).

Empirical filtration factors for Ar, O, and N are also shown in Fig. 1, and in all cases Models 2 and 8 results are consistent with the predicted range of values (when uncertainties are included). Model 18 is not consistent with theoretical calculations suggesting $F_{He} \sim 1$, but is consistent with Ar, O, and N predicted filtrations. Models 2 and 8 provide the best fit to the combined interstellar (Mg and C, FS03) and heliospheric data, and predict similar boundary conditions for the heliosphere ($n(H^{\circ})\sim 0.21\text{ cm}^{-3}$, $n(e^{-})\sim 0.10\text{ cm}^{-3}$, see Table 1). The radiative transfer models are not well constrained using heliospheric data alone. The semi-empirical filtration factors predicted by Models 2, 8 are, respectively: H (0.46 ± 0.05 , 0.47 ± 0.05), He (0.95 ± 0.09 , 1.06 ± 0.10), N (0.91 ± 0.17 , 0.93 ± 0.18), O (0.65 ± 0.10 , 0.67 ± 0.10), Ne (1.75 ± 0.34 , 2.34 ± 0.46), and Ar (1.10 ± 0.49 , 1.22 ± 0.554 , for Ar/H=3.16e-6, see below). The filtration factors based on Model 11 are within the range quoted for Model 2, although the uncertainties differ.

The result that $F_{Ne} > 1$ indicates that either the interstellar Ne abundance is poorly understood, or that a heliosheath process enhances Ne° (such as charge exchange with He° , with a similar ionization potential). The poorly understood extreme ultraviolet radiation field (570–790 Å, EUV) ionizes both Ne° and He° , and since He° data are consistent with model predictions, uncertainties in the EUV radiation field do not appear as the likely expla-

nation. The interstellar Ar abundance is uncertain (Sofia & Jenkins, 1998), and the abundance $\text{Ar}/\text{H}=3.16\text{e-}6$ is adopted here.

As a consistency check, the ratio of the PUI $n(\text{O})/n(\text{N})$ to the ISM $N(\text{O})/N(\text{N})$ values have been calculated, and compared to the ratio $F_{\text{O}}/F_{\text{N}}$. For the ISM, the ratio $N(\text{O}^{\circ})/N(\text{N}^{\circ})$ towards ϵ CMa is used (SF02, Gry & Jenkins 2001) (although this is not equal in detail to $n(\text{O}^{\circ})/n(\text{N}^{\circ})$ at the solar location because N° has a higher photoionization cross section than O°). The results are: $(n(\text{O})/n(\text{N})_{\text{pui}})/(N(\text{O})/N(\text{N})_{\text{ism}}) = 0.70\pm 0.28$, compared to $F_{\text{O}}/F_{\text{N}}=0.72\pm 0.20$, as expected.

4. 2 kHz Radio Emission

Gurnett et al. (1998, 2003) have detected a relatively isotropic radio-emission signal at 2 kHz in the outer heliosphere with the plasma wave instruments on board the two Voyager spacecraft; a possible explanation for the isotropy is emission at the plasma frequency of the surrounding interstellar gas providing this emission can enter the heliosphere (e.g. Izmodenov et al. 1999). If this emission has an interstellar origin, $n(e^{-})\sim 0.05\text{ cm}^{-3}$ and the closest match to this electron density among the SF02 models would be Model 25 ($n(e^{-})\sim 0.0607\text{ cm}^{-3}$) and Model 20 ($n(e^{-})\sim 0.0618\text{ cm}^{-3}$). Model 25 predicts: $n(\text{H}^{\circ})=0.21\text{ cm}^{-3}$, $n(\text{He}^{\circ})=0.017\text{ cm}^{-3}$, $\text{H}^{+}/\text{H}=0.194$, $\text{He}^{+}/\text{He}=0.341$ and $T=5,120\text{ K}$. Model 20 predicts: $n(\text{H}^{\circ})=0.23\text{ cm}^{-3}$, $n(\text{He}^{\circ})=0.018\text{ cm}^{-3}$, $\text{H}^{+}/\text{H}=0.183$, $\text{He}^{+}/\text{He}=0.346$ and $T=7,200\text{ K}$. The relatively low ionization levels found by these models results from the absence of a conductive interface on the cloud, which is characterized by the magnetic field parameter $B=0$. Model 25 yields predicted filtration factors of: $F_{\text{H}}=0.45\pm 0.05$, $F_{\text{He}}=0.85\pm 0.08$, $F_{\text{N}}=0.55\pm 0.11$, $F_{\text{O}}=0.39\pm 0.06$, $F_{\text{Ne}}=1.16\pm 0.23$, and $F_{\text{Ar}}=0.83\pm 0.37$. GG03 have found that Model 25 offers a self-consistent solution when heliosphere models of filtration are compared to the PUI data. However, if Model 25 is correct further study is required to understand the local ISM towards ϵ CMa, since the Model 25 predictions for interstellar abundances do not match the local ISM observations towards ϵ CMa.

5. Interstellar Magnetic Field

The interstellar magnetic field (B_{IS}) immediately outside of the heliosphere has not been directly measured. However, observations of weakly polarized light from nearby ($<50\text{ pc}$) stars show a patch of interstellar dust centered on galactic coordinates $l=350^{\circ}\rightarrow l=20^{\circ}$, $b=-40^{\circ}\rightarrow b=-5^{\circ}$, with extinction $A_{\text{V}}\sim 0.01\text{ mag}$ (or $N(\text{H})\sim 2\times 10^{19}\text{ cm}^{-2}$) and galactic field directed towards $l\sim 70^{\circ}$ (Tinbergen 1982, Frisch 1990). Fig. 2 shows the location of the stars (in galactic coordinates), and the polarization vectors, in the region where the weak polarization is most evident, with the plane of the ecliptic superimposed. Also plotted are the radio emission sources detected by the Voyager spacecraft which are consistent with an origin near the heliosphere nose and follow roughly the galactic plane (Kurth & Gurnett 2003). The weak polarization is most evident near the plane of the ecliptic and coincides with the upstream direction of the cluster of interstellar clouds flowing past the Sun (which is shown in Fig. 2 plotted in the Local Standard of Rest, after correction for solar motion). These polarizing dust grains are predominantly within 5 pc of the Sun, or closer (Frisch 1990). Although interstellar grain alignment mechanisms are poorly understood, popular grain alignment models

yield polarization vectors parallel to the interstellar magnetic field (Lazarian & Cho 2002). The same classical interstellar dust grains which polarize optical radiation also pile up in the heliosheath regions as grains are deflected around the heliosphere (grain radius $\sim 0.1 \mu\text{m}$, Frisch et al. 1999). Rand & Lyne (1994) compared pulsar dispersion and rotation measures towards pulsars spaced over several kpc, to derive the strength of the ordered component of the magnetic field near the Sun, $B=1.4\pm 0.2 \mu\text{G}$, directed towards galactic longitude $l = 88^\circ \pm 5^\circ$; this field is consistent with the field traced by Tinbergen's data. Once the production mechanisms for the grain alignment and for the radio emission sources are understood, it may produce a deeper understanding of the asymmetries in the heliosphere nose region due to the $\sim 60^\circ$ tilt between the ecliptic plane and interstellar magnetic field.

6. Variability in the Boundary Conditions of the Heliosphere.

Simple geometrical assumptions indicate the Sun left the Local Bubble interior and entered the surrounding interstellar cloud within the past several thousand years (Frisch 1994). More precise estimates of the variability of the boundary conditions of the heliosphere result from combining densities from the best RT models with observations of nearby stars.

Models 2 and 8 give a local ISM density of $n(\text{H}^\circ) \sim 0.21 \text{ cm}^{-3}$, which when combined with the column density to the cloud surface ($N(\text{H}^\circ) = 6.5 \cdot 10^{17} \text{ cm}^{-2}$) give a distance to the cloud surface of $\sim 0.97 \text{ pc}$. This distance is traversed in $\sim 37,000$ years by a cloud at the LIC velocity. Since the local ISM towards $\epsilon \text{ CMa}$ and $\alpha \text{ CMa}$ (Sirius) consists of two cloudlets (Gry & Jenkins 2001, Lallement et al. 1994), and the second blue-shifted cloud has a higher velocity relative to the Sun than the LIC, the time at which the Sun encountered the LIC must be shorter than 37,000 years. Frisch (1997) attributed spikes in the ^{10}Be ice core record 33 kyr and 60 kyr ago to encounters with $\sim 0.1 \text{ pc}$ wide magnetic structures, comoving in the local ISM, which confine low energy galactic cosmic rays. These structures would now be $\sim 0.87 \text{ pc}$, and $\sim 1.6 \text{ pc}$ distant from the Sun in the downstream direction (e.g. towards $\epsilon \text{ CMa}$, $\alpha \text{ CMa}$). The most recent ^{10}Be spike may be consistent with the solar entry into the local ISM; alternatively it may correlate with the Sun's entry into the LIC while the earlier event may signal entry into the blue-shifted cloud seen towards CMa. Prior to that, the Sun was immersed in the hot (10^4 K) plasma interior to the Local Bubble where an extended heliosphere (heliopause radius 300 au in the nose direction) is predicted (Frisch et al. 2003). (Civilization developed as the Sun emerged from the Local Bubble interior, where it resided for several millions of years.)

Looking to the future, at least three interstellar clouds are found within 5 pc of the Sun in the upstream direction, the Local Interstellar Cloud (LIC) where the Sun is now located, the "G-cloud", and the Apex Cloud (Frisch 2003). The velocity vector of each cloud is consistent with the cloud being located in front of the nearest star $\alpha \text{ Cen}$, although the G-cloud is the best fit to observations (e.g. Lallement et al. 1995, Linsky & Wood 1996) and the LIC would have to have a small velocity gradient ($\sim 0.7 \text{ km/s}$) towards the star. If the G-cloud is the next cloud to be encountered by the Sun, the higher heliocentric velocity (-29.1 km/s , factor of ~ 1.1) and neutral density ($> 5 \text{ cm}^{-3}$, factor of > 24) than for the LIC indicates a dramatic heliosphere shrinkage if the other properties (e.g. ionization) are similar to the LIC (Frisch 2003, Zank &

Frisch 1999). If, in contrast, the Apex Cloud is the next cloud encountered, the larger heliocentric velocity (-35.1 km s^{-1}) also indicates a smaller heliosphere, although the other properties of this cloud are unknown. Variations of the boundary conditions of the heliosphere are thus expected on timescales of less than 37,000–45,000 years if either the G-cloud or Apex Cloud is foreground to $\alpha \text{ Cen}$.

7. Discussion

The primary results of this paper are estimates of filtration factors for H, He, N, O, Ne, and Ar, based on radiative transfer models of the local ISM from SF02, and FS03. Two radiative transfer equilibrium models of ISM within $\sim 3 \text{ pc}$ of the Sun (models 2 and 8) yield predictions which match observations of ISM inside (He, PUIs, ACRs) and outside (gas within $\sim 3 \text{ pc}$ towards $\epsilon \text{ CMa}$) of the solar system, for an assumed interstellar gas-phase O abundance of $\text{O}/\text{H}=400 \text{ ppm}$ (FS03). These models yield semi-empirical predictions for He, H, O, N, Ar filtration factors which are consistent with theoretical predictions, within uncertainties, and predict interstellar densities $n(\text{H}^{\circ})\sim 0.20 \text{ cm}^{-3}$, $n(e^{-})=0.10 \text{ cm}^{-3}$ at the solar location. However, there are unexplained differences between the predictions of Models 2 and 8 and observed pickup ion Ne densities and the cloud temperature.

If the astronomical constraints on the radiative transfer models are relaxed, alternate models become plausible. For example, if the 2 kHz radio emission observed by Voyager 1, 2 is from the surrounding ISM, the low electron density of Model 25 ($n(e^{-})\sim 0.06 \text{ cm}^{-3}$) is a better match although predicted interstellar abundances are unrealistic. For Model 25 to be correct the radiation field intensity versus cloud geometry requires further study. The simple interstellar cloud geometry assumed for the underlying radiative transfer models may also prove inadequate. If the astronomical constraints prove incorrect (e.g. the assumed interstellar gas-phase oxygen abundance), then the selection of the best models to describe the boundary conditions of the heliosphere may also change.

As better data on the ISM inside and outside of the heliosphere become available, yielding more accurate boundary conditions for the heliosphere, heliosphere modeling will predict more reliable filtration factors for comparison with semi-empirical filtration factors utilizing interstellar modeling.

The strength of the interstellar magnetic field outside of the heliosphere remains uncertain, but both low frequency radio emission events and the polarization of the light of nearby stars suggest the field orientation is parallel to the galactic plane and not the ecliptic plane, introducing a north/south heliosphere asymmetry.

The second important conclusion of this paper is that the boundary conditions of the heliosphere change with time, and on timescales of $<10^4$ years, indicating past and future variations in heliosphere dimensions and properties.

Acknowledgments. The author acknowledges research support from NASA grants NAG5-6405, and NAG5-11005, and NAG5-8163. The author would like to thank the referees for helpful comments which improved this paper.

8. References

- Andre, M., C. Oliveira, J. C. Howk, R. Ferlet, J. M. Desert, G. Hebrard, S. Lacour, A. Lecavelier des Etangs, A. Vidal-Madjar, and H. W. Moos, Oxygen gas phase abundance revisited, *Astrophys. J.*, , p. submitted, 2002.
- Cheng, K. and Bruhweiler, F. C., Ionization Processes in the Local Interstellar Medium - Effects of the Hot Coronal Substrate, *Astrophys. J.*, 364, 573–581, 1990.
- Cummings, A. C., E. C. Stone, and C. D. Steenberg, Composition of Anomalous Cosmic Rays and Other Heliospheric Ions, *Astrophys. J.*, 578, 194–210, 2002.
- Frisch, P. C., Characteristics of the local interstellar medium, in *Physics of the Outer Heliosphere*, pp. 19–22, 1990.
- Frisch, P. C., Journey of the Sun, <http://xxx.lanl.gov/astro-ph/970523>, 1997.
- Frisch, P. C., Morphology and ionization of the interstellar cloud surrounding the solar system, *Science*, 265, 1423, 1994.
- Frisch, P. C., Local Interstellar Matter: The Apex Cloud, *Astrophys. J.*, *in press*, 2003.
- Frisch, P. C., and J. D. Slavin, Chemical Composition and Gas-to-Dust Mass Ratio of the Nearest Interstellar Matter, *Astrophys. J.*, *in press*, 2003.
- Frisch, P. C., J. M. Dorschner, J. Geiss, J. M. Greenberg, E. Grün, M. Landgraf, P. Hoppe, A. P. Jones, W. Krätschmer, T. J. Linde, G. E. Morfill, W. Reach, J. D. Slavin, J. Svestka, A. N. Witt, and G. P. Zank, Dust in the Local Interstellar Wind, *Astrophys. J.*, 525, 492–516, 1999.
- Frisch, P. C., L. Grodnicki, and D. E. Welty, The Velocity Distribution of the Nearest Interstellar Gas, *Astrophys. J.*, 574, 834–846, 2002.
- Frisch, P. C., H. R. Mueller, G. P. Zank, and C. Lopate, Galactic Environment of the Sun and Stars: Interstellar and Interplanetary Material, in *Astrophysics of Life*, Eds. M. Livio, I. N. Reid, and W. B. Sparks (Cambridge: Cambridge University Press), 2003.
- Gloeckler, G., and J. Geiss, Composition of the Local Interstellar Cloud from Observations of Interstellar Pickup Ions, in *AIP Conf. Proc. 598: Joint SOHO/ACE workshop "Solar and Galactic Composition"*, pp. 281–+, 2001.
- Gloeckler, G., and J. Geiss, Composition of the Local Interstellar Cloud as Diagnosed with Pickup Ions, *Adv. Space Res.*, *in press*, 2003.
- Gry, C., and E. B. Jenkins, Local clouds: Ionization, temperatures, electron densities and interfaces, from GHRS and IMAPS spectra of epsilon Canis Majoris, *Astron. Astrophys.*, 367, 617–628, 2001.
- Izmodenov, V. V., J. Geiss, R. Lallement, G. Gloeckler, V. B. Baranov, and Y. G. Malama, Filtration of interstellar hydrogen in the two-shock heliospheric interface: Inferences on the local interstellar cloud electron density, *J. Geophys. Res.*, 104, 4731–4742, 1999.
- Kimble, R. A., Davidsen, A. F., Blair, W. P., Bowers, C. W., Dixon, W. V. D., Durrance, S. T., Feldman, P. D., Ferguson, H. C., Henry, R. C., Kriss, G. A., Kruk, J. W., Long, K. S., Moos, H. W., Vancura, O., Extreme Ultraviolet Observations of G191-B2B and the Local Interstellar Medium with the Hopkins Ultraviolet Telescope, *Astrophys. J.*, 404, 663–672, 1993.
- Kurth, W. S., and D. A. Gurnett, On the source location of low-frequency heliospheric radio emissions, *J.*

Geophys. Res., *this issue*, 000, 2003.

- Lallement, R., Bertin, P., Ferlet, R., Vidal-Madjar, A., and Bertaux, J., GHRs observations of Sirius-A I. Interstellar clouds toward Sirius and Local Cloud ionization, *Astron. Astrophys.*, *286*, 898–908, 1994.
- Lallement, R., R. Ferlet, A. M. Lagrange, M. Lemoine, and A. Vidal-Madjar, Local cloud structure from HST-GHRs, *Astron. Astrophys.*, *304*, 461–474, 1995.
- Linsky, J. L., and B. E. Wood, The alpha Centauri line of sight: D/H ratio, physical properties of local interstellar gas, and measurement of heated hydrogen (the ‘hydrogen wall’) near the heliopause, *Astrophys. J.*, *463*, 254–270, 1996.
- Lazarian, A., and J. Cho, Polarized Foreground Emission from Dust: Grain Alignment and MHD Turbulence, *Elsevier Science*, submitted, 2002.
- Mueller, H., and G. P. Zank, Modeling Heavy Ions and Atoms throughout the Heliosphere, in *“Solar Wind 10”*, 2002.
- Rand, R. J., and A. G. Lyne, New Rotation Measures of Distant Pulsars in the Inner Galaxy and Magnetic Field Reversals, *Mon. Not. R. Astron. Soc.*, *268*, 497–+, 1994.
- Ripken, H. W., and H. J. Fahr, Modification of the local interstellar gas properties in the heliospheric interface, *Astron. Astrophys.*, 1983.
- Slavin, J. D., Consequences of a Conductive Boundary on the Local Cloud, *Astrophys. J.*, *346*, 718–727 1989.
- Slavin, J. D., and P. C. Frisch, The Ionization of Nearby Interstellar Gas, *Astrophys. J.*, *565* 364–379, 2002.
- Sofia, U. J., and E. B. Jenkins, Interstellar medium absorption profile spectrograph observations of interstellar neutral argon and the implications for partially ionized gas, *Astrophys. J.*, *499* 591, 1998.
- Tinbergen, J., Interstellar polarization in the immediate solar neighborhood, *Astron. Astrophys.*, *105*, 53–64, 1982.
- Vallergera, J., Observations of the Local Interstellar Medium with the EUVE, *Space Science Reviews*, *78*, 277–288, 1996.
- Witte, M., M. Banaszekiewicz, H. Rosenbauer, and D. McMullin, Kinetic parameters of interstellar neutral helium: Updated results from the ULYSSES/GAS instrument, *Adv. Space Res.*, *in press*, 2003.
- Zank, G. P. and Frisch, P. C., Consequences of a Change in the Galactic Environment of the Sun, *Astrophys. J.*, *518*, 965–973, 1999.

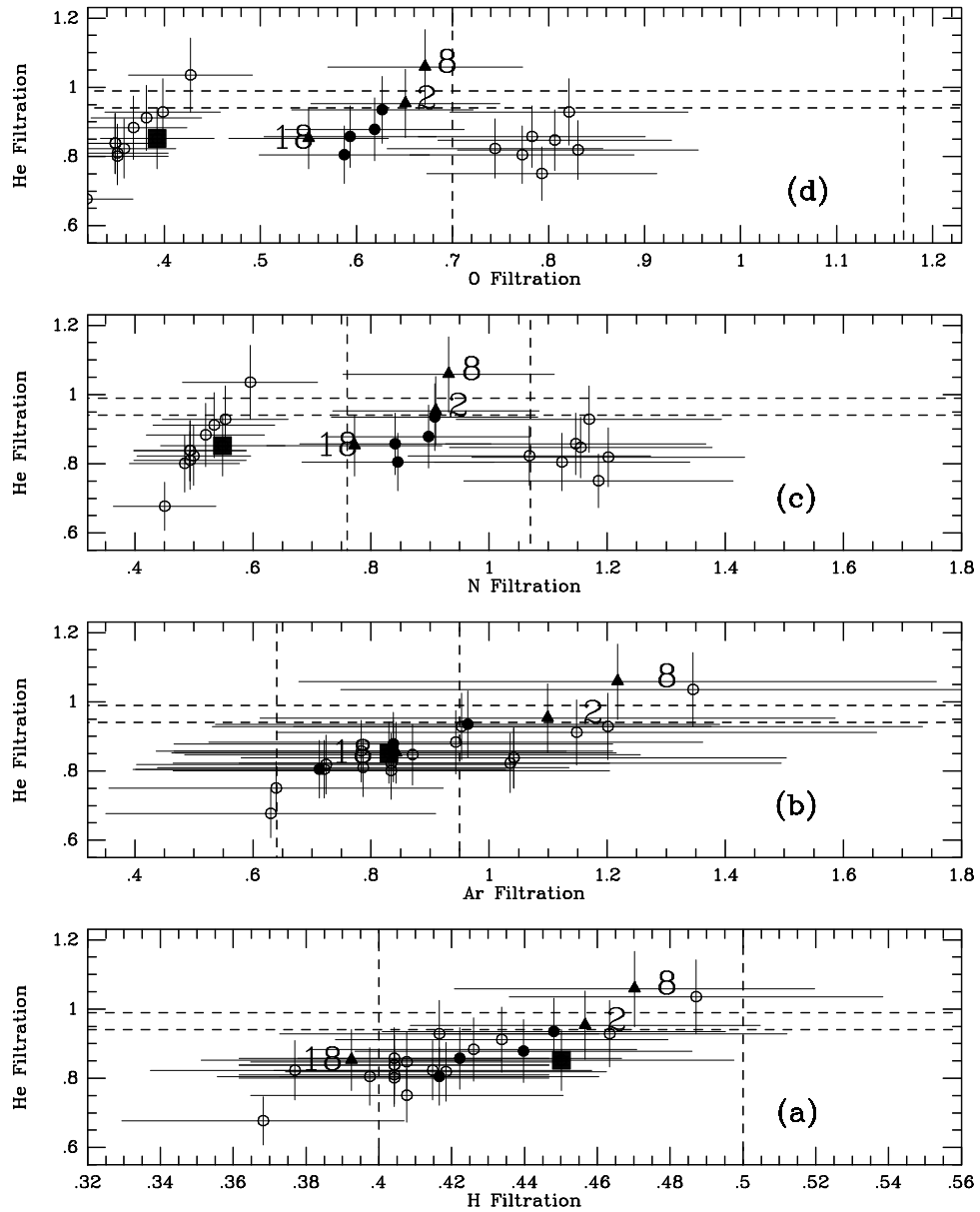


Figure 1. Empirical filtration factors for H (a), Ar (b), N (c), and O (d) are plotted against F_{He} , as derived from RT models (SF02, Table 7) compared to PUI, ACR, and He data (including data uncertainties). Filled circles and triangles are ISM models with $\text{O}/\text{H} \sim 400$, and the labeled triangles are nos. 2, 8, 18 which match local ISM Mg^+/Mg^0 and C^+/C^{+*} data. The box shows Model 25 (consistent with a low electron density). Dashed lines are theoretical filtration factors.

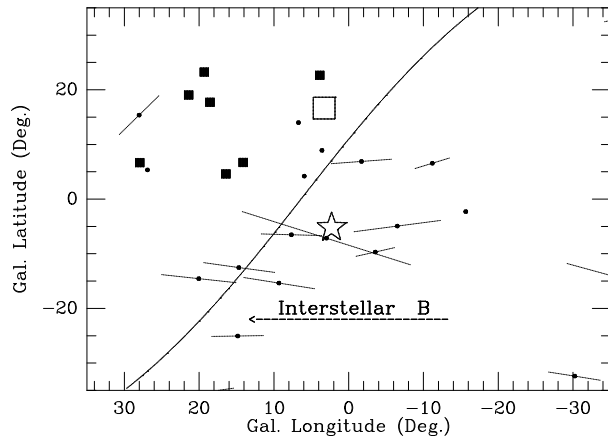


Figure 2. Plot of an indicator of the nearby interstellar magnetic field, in galactic coordinates. The bars show the direction of the electric vector polarization, which is parallel to the interstellar magnetic field direction, for several nearby stars (Tinbergen 1982). The arrow shows the likely direction of the interstellar magnetic field near the Sun based on the polarization and pulsar (Rand & Lyne 1994) data. The curved line is the ecliptic plane. The observed region of maximum polarization is near the ecliptic plane, but is also in the upstream direction (as referred to the “LSR” velocity rest frame of stars close to the Sun, Frisch et al. 2002) of the local flow of ISM past the Sun (star). The heliosphere nose direction, in the heliocentric rest frame, is located at the box. For comparison, the sources determined for the ~ 3 kHz radio emissions detected by Voyager are plotted as filled boxes (Kurth & Gurnett 2003).

Table 1. ISM Physical Properties at the Heliosphere^a

Quantity	Models	
	2	8
<i>Assumed Model Parameters</i>		
n_{H} (cm ⁻³) ^b	0.273	0.273
log T_{h} (K)	6.0	6.1
B_{o} (μG)	5.0	5.0
$N_{\text{H}^{\circ}}$ (10 ¹⁷ cm ⁻²) ^c	6.5	6.5
<i>Predicted Quantities at Solar Location</i>		
$n(\text{H}^{\circ})$ (cm ⁻³)	0.208	0.202
$n(\text{He}^{\circ})$ (cm ⁻³)	0.015	0.014
$n(\text{e})$ (cm ⁻³)	0.098	0.101
$\chi(\text{H})$ ^d	0.287	0.300
$\chi(\text{He})$ ^d	0.471	0.511
T (K)	8,230	8,480
$n(\text{N}^{\circ})/n(\text{He}^{\circ})$	5.64e-4	6.12e-4
$n(\text{O}^{\circ})/n(\text{He}^{\circ})$	5.35e-3	5.76e-3
$n(\text{Ne}^{\circ})/n(\text{He}^{\circ})$	3.86e-4	2.37e-4
$n(\text{Ar}^{\circ})/n(\text{He}^{\circ})$ ^e	1.21e-5	1.21e-5
<i>Predicted Quantities towards ϵ CMa</i>		
log N_{H} (cm ⁻²) ^{b,c}	18.03	18.02
$N(\text{H}^{\circ})/N(\text{He}^{\circ})$ ^c	11.63	12.74

^a From (Slavin & Frisch 2002) and (Frisch & Slavin 2002).^b $n_{\text{H}} = n(\text{H}^{\circ}) + n(\text{H}^{+})$ cm⁻³; $N_{\text{H}} = N(\text{H}^{\circ}) + N(\text{H}^{+})$ cm⁻².^c $N(\text{H}^{\circ})$ is the H^o column density between the Sun and cloud surface, etc., where the cloud is the sum of the two nearby cloudlets ($d < 3$ pc) observed towards ϵ CMa (Gry & Jenkins 2001).^d $\chi(\text{H})$, $\chi(\text{He})$ are the ionized fractions of H, He, respectively.^e The B-star Ar abundance of 3.16 ppm is used here (from Sofia & Jenkins 1998).